Molecular Crystals and Liquid Crystals
Publication details, including instructions for authors and subscription information:
http://www.tandfonline.com/loi/gmcl16

EPR and Optical Absorption Studies of γ-irradiated Pyrene Single Crystals

Tetsuya Kawakubo [a]

[a] Research Reactor Institute, Kyoto University, Kumatori-cho, Sennan-gun, Osaka, Japan

To cite this article: Tetsuya Kawakubo (1978): EPR and Optical Absorption Studies of γ-irradiated Pyrene Single Crystals, Molecular Crystals and Liquid Crystals, 46:1-2, 11-24

To link to this article: http://dx.doi.org/10.1080/00268947808084842

Mol. Cryst. Liq. Cryst., 1978, Vol. 46, pp. 11-24

Printed in Holland

EPR and Optical Absorption Studies of γ-irradiated Pyrene Single Crystals

TETSUYA KAWAKUBO
Research Reactor Institute, Kyoto University, Kumatori-cho, Sennan-gun, Osaka, Japan

(*Received September 27, 1977; in final form January 25, 1978*)

Pyrene single crystals irradiated with γ rays at room temperature have been investigated by electron paramagnetic resonance and optical absorption experiments. EPR spectra exhibit a triplet characteristic and each line of the triplet shows characteristic features with rotations of the crystals in a magnetic field. From analyses of these spectra the presence of two kinds of hydrogen added pyrene radicals, 3-H_2-pyrene and 2-H_2-pyrene radicals, is concluded. In the optical absorption spectrum nine main absorption bands have been detected. These absorption bands are compared with the theoretically calculated transition energies with SCF-CI molecular orbital calculations for 3-H_2-pyrene and 2-H_2-pyrene radicals. Reasonable correspondences are obtained between theoretical values and the experimental spectrum.

1 INTRODUCTION

EPR and optical investigations of the effects of ionizing radiation on the aromatic hydrocarbons, such as benzene, naphthalene, and anthracene have revealed that stable hydrogen added radicals are produced in the crystals. However, detailed analysis of the irradiation products in single crystals of aromatics has been made only in the case of naphthalene[1,2] and anthracene[3,4]. Pyrene is one of the most representative of the aromatics and its physical and chemical properties have been studied extensively. In this paper analyses of EPR and optical absorption spectra of irradiated pyrene single crystals are reported.

2 EXPERIMENTAL

Pyrene was dissolved in benzene and purified through columns of alumina and silica gel at a length of 20 m and then zone refined by 100 passes. Crystals were grown by the Bridgman technique in an evacuated cell. Single crystals

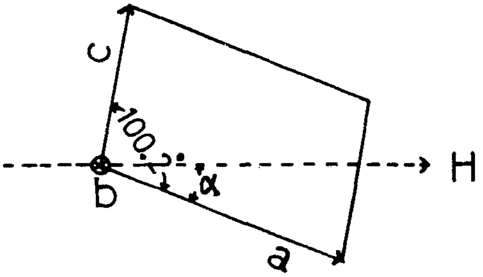

FIGURE 1 A unit cell of pyrene crystals and the direction of the magnetic field.

of 3 × 5 × 8 mm^3 for use in the EPR study and 7 × 7 × 2 mm^3 for optical measurements were irradiated at room temperature with γ-rays up to a dose of 3 × 10^7 rad. Crystals were set in a magnetic field with the *b*-axis perpendicular to the field and were rotated around the *b*-axis. EPR measurements were made at room temperature using a microwave frequency of approximately 9.5 GHz and a power of 0.2 mW. Setting of the crystal in the magnetic field is illustrated in Figure 1. Optical absorption spectra were measured at room temperature.

3 RESULTS AND DISCUSSION

3.1 EPR spectra

Typical angular dependence of the EPR spectrum is shown in Figure 2, where the angle α between the direction of the magnetic field and the *a*-axis is denoted. The spectrum at each angle exhibits a broad triplet. Since such a line profile is very similar to that of the radicals in other aromatics,[1,8,9] this triplet is considered to be due to hydrogen added radical. The intensity of the central line of the triplet relative to the other lines is greater than that determined by the ratio 1:2:1 of a triplet. This intensity ratio suggests the presence of more than one type of radical. Each spectrum in Figure 2 exhibits a characteristic feature with rotations. Fine structures with a separation of 2 gauss are observed clearly at $\alpha = 70°$ and disappear completely at around $\alpha = 130°$. The spectrum at $\alpha = 150°$ has a structure with a separation of 5 gauss. In the case of $\alpha = 0° \sim 20°$, there is no regular fine splitting. The spectrum at $\alpha = 30°$ has a fine structure of 2 gauss only for the line at the center of the main triplet. The difference in the splitting of the central lines of triplet and that of the side lines is considered to indicate the presence of two kinds of triplet spectra whose splitting are different from each other.

It is well known that the carbon site with the highest chemical activity in the pyrene molecule is at position 3 and that with the next activity is at

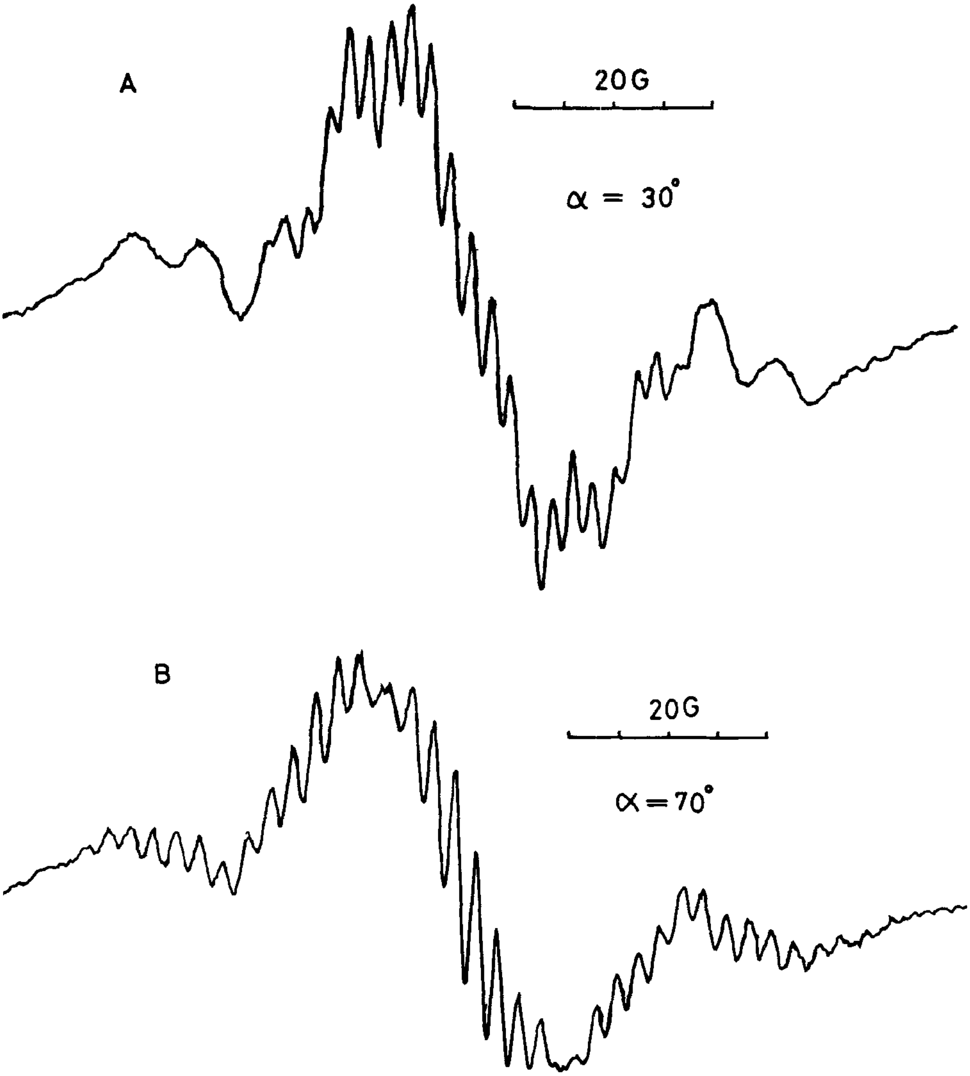

FIGURE 2 EPR spectra of pyrene single crystal irradiated by γ-rays. A) $\alpha = 30°$, B) $\alpha = 70°$, C) $\alpha = 130°$, D) $\alpha = 150°$. α denotes the angle between the magnetic field and a-axis.

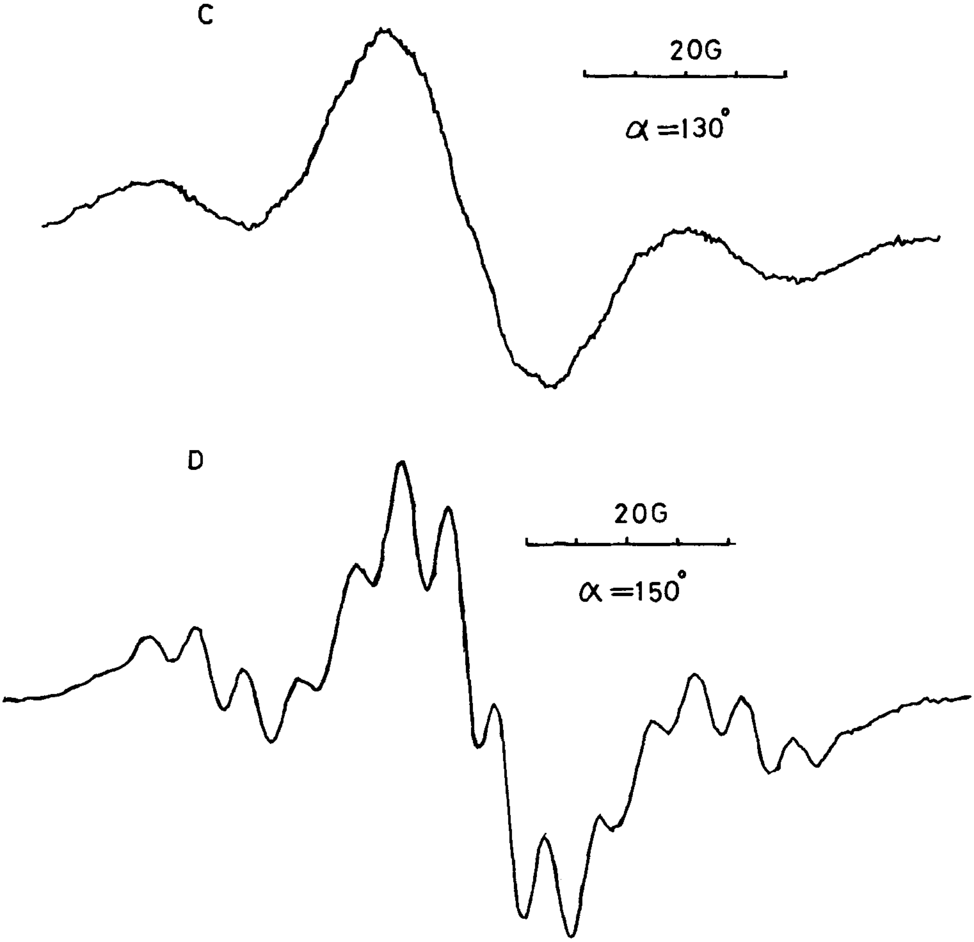

FIGURE 2 (*continued*)

position 2. In the analysis of pyrenium ion,[6] the species with an additional proton to these two positions in a pyrene molecule have been considered. We analyze the EPR spectra assuming the presence of two kinds of radicals; one is a radical having an additional hydrogen atom at position 3, the other is one having hydrogen atom at position 2. In analyzing these complex spectra we use the following method. First, the spin densities are calculated theoretically. Using the principal value of the hyperfine tensor of an α-proton, which was obtained from an analysis of the EPR spectrum of hydronaphthyl radical,[2] we calculated the semi-empirical hyperfine splitting. Neglecting the influence of the spin on the next nearest neighbour atom, these hyperfine

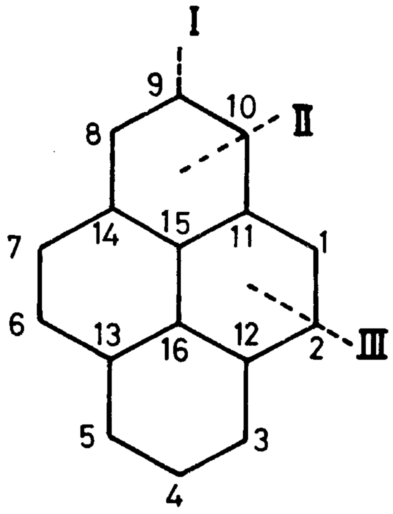

FIGURE 3 Site number and direction number.

constants can be utilized in our case. Then the calculated spectrum is compared with the experimental spectrum. McLachlan's method was applied to calculate spin densities. The H_2 in the CH_2 group was treated as a heteroatom model with the parameters: $h_{H_2} = -1.0$, $h_c = 0.3$, $k_{c\text{-}H_2} = 2.6$. These constants have given reasonable spin densities for cyclohexadienyl and hydronaphthyl radicals.[7] Calculated spin densities of 3-H_2-pyrene and 2-H_2-pyrene radicals are shown in Figure 4. The 2-H_2-pyrene radical has a carbon atom with a high spin density of 0.6 while the spin distribution in 3-H_2-pyrene is nearly uniform over a molecule. The hyperfine splitting due to the α-proton is expressed as

$$A = \rho\sqrt{A_x L_x^2 + A_y L_y^2 + A_z L_z^2}$$

where A_x, A_y, and A_z are the principal values of the hyperfine tensor of the α-proton, ρ the spin density and L_x, L_y, and L_z, the direction cosines. Using the value of $A_x = -13$, $A_y = -42$, and $A_z = -30$ gauss, the angular dependence of A/ρ at positions I, II and III (see Figure 3) are obtained. For the broad triplet due to the methylene group, the value of A/ρ was taken to be 353[7] gauss and splittings obtained were 26.2 gauss for 3-H_2-pyrene and 28.7 gauss for 2-H_2-pyrene, respectively. The value of A/ρ for an α-proton coupling are shown in Table I. We may find some correlations between the value of A/ρ and the characteristic features of the EPR spectra. At $\alpha = 150°$ the value of A/ρ is the same for positions II and III and the spectrum splits by 5 gauss. At $\alpha = 120° \sim 130°$ A/ρ of II is two times as large as that of III and the spectrum has no structure. From the value of A/ρ and spin densities

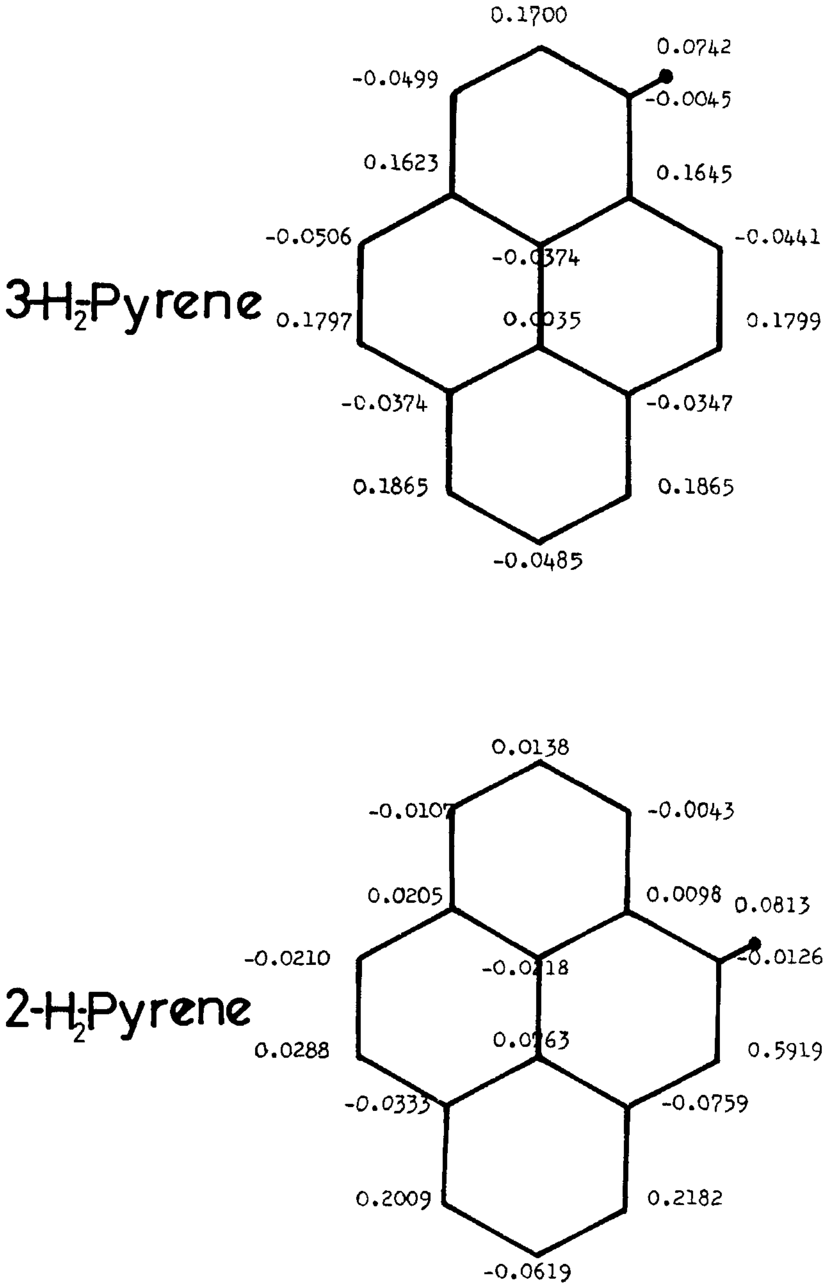

FIGURE 4 Calculated spin density.

TABLE I

Values of A/ρ and the characteristic features of the spectra.

	A/ρ (gauss)			
α	I	II	III	Characteristic features of the spectra
30°	21.1	29.6	39.1	Fine structure is observed only in the central region
70°	16.7	40.7	31.0	2 gauss splitting
120°	34.6	36.5	18.0	No fine structure
130°	36.6	33.4	19.7	
150°	37.8	26.5	26.3	5 gauss splitting

in the case of $\alpha = 150°$, the calculated splitting is obtained and shown in Table II and Figure 5. Correspondence between experimental fine structure and the calculated ones is reasonable. To arrange the intensity distribution of the spectrum, the relative concentration of 2-H_2-pyrene to 3-H_2-pyrene is necessary. The intensity distribution, in the case that the ratio of total intensity of each line is equal for the two radicals, is shown in Figure 6. In this figure the splittings of the triplet due to the methylene group are taken to 26.2 and 28.7 gauss for 3- and 2-H_2-pyrene, respectively. The positions of the lines of the 2-H_2-pyrene coincide with that of the 3-H_2-pyrene in the center line of the broad triplet, but in the side lines of the triplet the spectral lines of one radical are located in the middle of the lines of the other radical. Consequently, the intensity is large in the center of the broad triplet. However, the relative intensity of the center line to the side lines in the experimental spectrum is still larger than that of the calculated spectrum. If we assume the presence of a singlet like signal at the center line of the triplet, then this problem about the intensity ratio of each line of the triplet is solved. It is adequate to consider that this signal comes from hydrogen subtracted pyrene radicals[4,5,8] which do not recombine in the crystal even at room temperature.

TABLE II

Calculated hyperfine splittings for the α-proton coupling at $\alpha = 150°$.

		Position			
		I	II	III	Spin density
A/ρ (gauss)		37.8	26.5	26.3	
Splitting (gauss)	3-H_2-pyrene		4.8	4.7	0.18
		6.4			0.17
	2-H_2-pyrene		15.9	15.8	0.6
			5.3	5.3	0.2

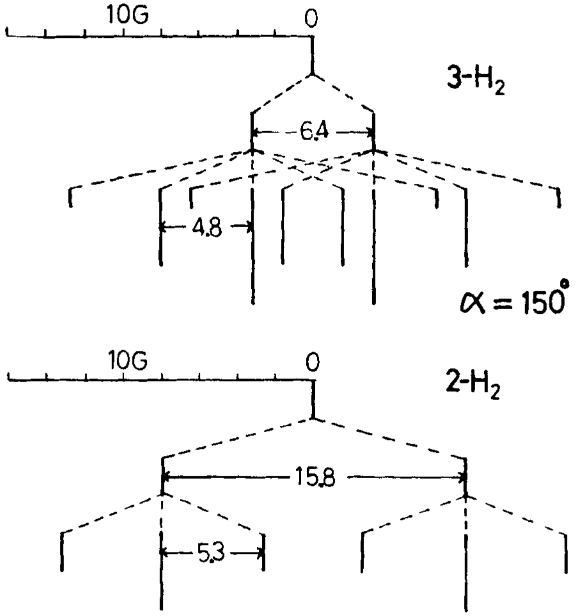

FIGURE 5 Assignments of the EPR spectra for the 3-H_2-pyrene and the 2-H_2-pyrene radicals at $\alpha = 150°$.

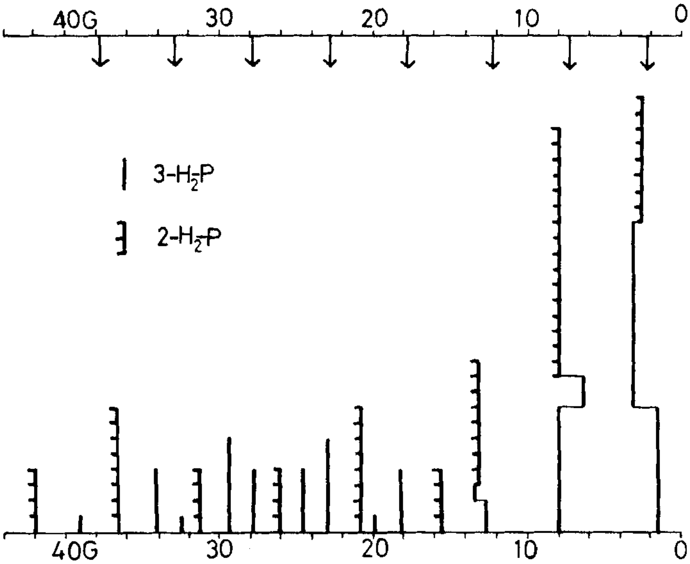

FIGURE 6 Theoretical distribution of the EPR lines. Arrows indicate experimental line positions.

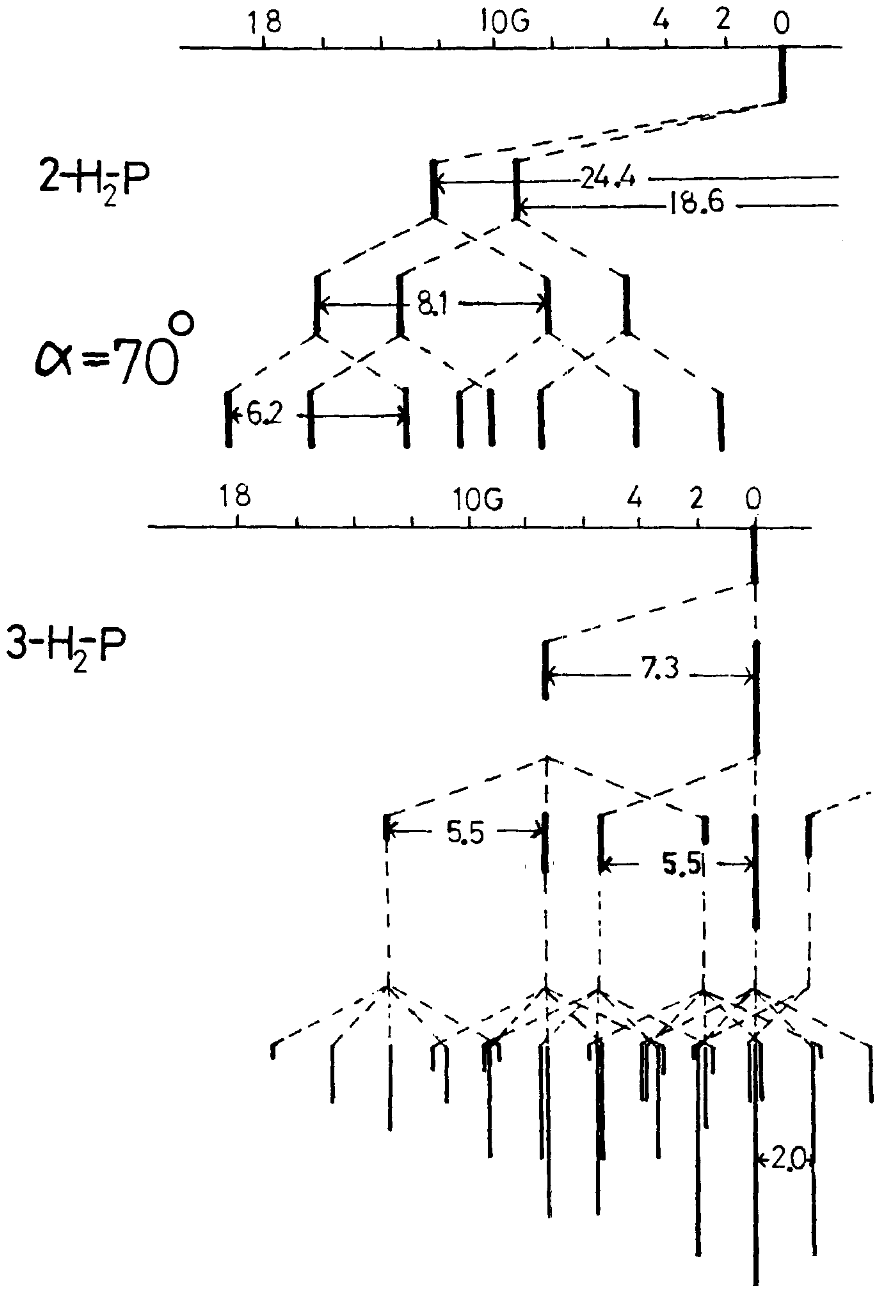

FIGURE 7 Assignments of the EPR spectra for the 3-H_2-pyrene and the 2-H_2-pyrene radicals at $\alpha = 70°$.

TABLE III

Calculated hyperfine splittings for the α-proton coupling at $\alpha = 70°$.

		Position			
		I	II	III	Spin density
A/ρ (gauss)		16.7	40.7	31.0	
Splitting (gauss)	3-H_2-pyrene		7.3	5.5	0.18
		2.8			0.17
			2.0	1.6	0.05
	2-H_2-pyrene		24.4	18.6	0.6
			8.1	6.2	0.2

In the case of $\alpha = 70°$ the calculated splittings and spectra of 3-H_2-pyrene and 2-H_2-pyrene are shown in Table III and in Figure 7. In the spectrum of 3-H_2-pyrene, splittings of 2.8, 2.0 and 1.6 gauss are drawn as 2.00 gauss for simplicity. The spectrum of 3-H_2-pyrene has lines separated by 2 gauss. On the other hand the spectrum of 2-H_2-pyrene has no regular splitting of 2 gauss, however these lines do not necessarily disturb the structure of 2 gauss. Asymmetric structure concerning the position of the lines in the experimental spectra may suggest small differences in the g-value and its angular dependence in the two types of radicals.

We have compared the semi-empirically calculated spectra with the experimental ones and obtained fairly good agreement. This fact proves the formation of 2-H_2-pyrene and 3-H_2-pyrene by irradiation of pyrene crystals.

3.2 Optical absorption spectra

The optical absorption spectra of pyrene single crystals irradiated with γ-rays at room temperature are shown in Figure 8. Main absorption bands are detected at 398 mμ, 417, 435, 487, 530, 550, 580, 618, 680 mμ, respectively. Since the results obtained from analysis of the EPR spectra indicate the existence of 3-H_2-pyrene and 2-H_2-pyrene radicals, in order to analyze the optical spectra we consider the correspondence of the absorption bands in the experimental spectra of the theoretical spectra of 3-H_2-pyrene and 2-H_2-pyrene radicals. Theoretical spectra of hydrogen added benzene and naphthalene radicals[7] have been calculated and the agreement of the theoretical spectra with the experimental ones is reasonably good. The same method of calculation was applied to 3-H_2-pyrene and 2-H_2-pyrene radicals based on the semi-empirical method developed by Praiser and Parr, combined with the SCF method for an open shell developed by Longuet-Higgins and Pople. The H_2 unit of CH_2 in the radical is regarded as a pseudo

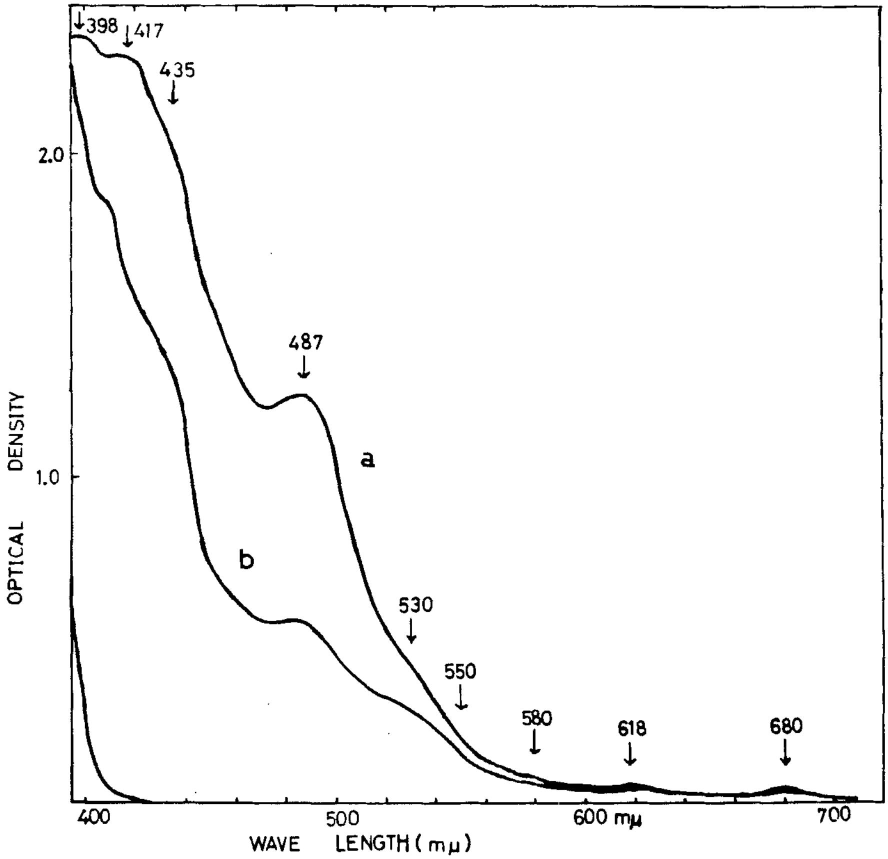

FIGURE 8 Optical absorption spectrum of a γ-irradiated pyrene single crystal.

atom. The ionization potential and electron affinity of the H_2-atom are taken to be 9.4219 eV and −0.7007 eV.[10] The overlap integral and the resonance integral between the pseudo π orbital of the H_2-atom and the adjacent carbon $2p\pi$ atomic orbital are 0.613 and −5.90 eV, respectively. Using these values SCF calculation was carried out for 17 electrons. Configuration interaction was considered among 19 lower energy configurations of radical doublet states. Results of the calculations for 3-H_2-pyrene and 2-H_2-pyrene radicals are shown in Table IV. The lowest transition of each radical corresponds to the configuration mixing state between the transition from the highest occupied orbital to the half filled orbital and the transition from the half filled one to the lowest vacant orbital. The energy of this lowest transition is lower in 3-H_2-pyrene than in 2-H_2-pyrene. The lowest absorption band of 680 mμ in the experimental spectrum may be assigned to this

TABLE IV

Theoretical electronic transitions in 3-H_2-pyrene and 2-H_2-pyrene radicals.

	Energy (eV)	Transition moment (Å)[a] Short-axis	Long-axis	Oscillator strength
3-H_2-pyrene	1.99	0.060	0.040	8.86×10^{-4}
	2.56	0.058	0.056	1.45×10^{-3}
	2.93	0.075	0.008	1.46×10^{-3}
	3.16	0.203	0.559	9.73×10^{-2}
	3.43	0.406	0.139	5.51×10^{-2}
2-H_2-pyrene	2.20	0.021	0.012	1.14×10^{-4}
	2.49	0.030	0.015	2.43×10^{-4}
	2.88	0.332	0.800	1.88×10^{-1}
	3.52	0.469	0.013	6.76×10^{-2}

[a] Absolute value.

lowest transition of 3-H_2-pyrene. Polarization rate of absorption intensity in the theoretical spectra is calculated assuming that the radical has the same orientation as the host molecule. Since the angle between short axis of the radical and the *a*-axis of the crystal is nearly equal to the corresponding value for the *b*-axis, the transition parallel to the short axis of the radicals causes equal intensity of absorption in the direction parallel to the *a*-axis and in that parallel to the *b*-axis. Therefore, the absorption intensity is always larger for the direction parallel to the *a*-axis than for that parallel to the *b*-axis. The next lowest absorption band with theoretical indication is the 2.20 eV band of 2-H_2-pyrene and in the case of 3-H_2-pyrene the next lowest absorption is the 2.56 eV band, so that the theoretical band at 2.20 eV may be taken to correspond to the 618 mμ band in the experimental spectrum. Similarly, considering the order of the energy and the magnitude of oscillator strength, we may correlate the experimental bands to the theoretical ones.

TABLE V

Orientation of the molecule in pyrene crystals (Ref. 11)

	Angle between long axis of molecule and *a*, *b*, *c'*-axis of crystals		Angle between short axis of molecule and *a*, *b*, *c'*-axis of crystals	
	ω	$\cos \omega$	ω	$\cos \omega$
a-axis	61.1°	0.4834	52.2°	0.6130
b	77.7	0.2130	52.4	0.6101
c'	31.9	0.8487	120.1	−0.5017

TABLE VI

Main optical absorption bands in γ-irradiated pyrene single crystals.

Experimental		Theoretical		
Wave length (mμ)	Photon energy (eV)	Transition energy (eV)	Oscillator strength	Assignment
680	1.82	1.99	8.86×10^{-4}	3-H_2-pyrene
618	2.01	2.20	1.14×10^{-4}	2-H_2-pyrene
580	2.14			?
550	2.25	2.49	2.43×10^{-4}	2-H_2-pyrene
530	2.34	2.56	1.45×10^{-3}	3-H_2-pyrene
487	2.54	2.88	1.88×10^{-1}	2-H_2-pyrene
435	2.85	2.93	1.46×10^{-3}	3-H_2-pyrene
417	2.97			
398	3.11			

These assignments are shown in Table VI. The weak absorption around 650 mμ may be supposed to be an absorption caused by a species such as the dimer radical.[4,5] For the assignment of these absorption bands experimental evidence is expected. Irradiation at low temperature and successive annealing experiments may be useful for the assignment of each absorption band.

We have examined the comparison of the experimental absorption bands with the theoretically calculated transition energies of 3-H_2-pyrene and 2-H_2-pyrene radicals and obtained consistent results. This fact endorses the adequacy of the assignments of the EPR spectra.

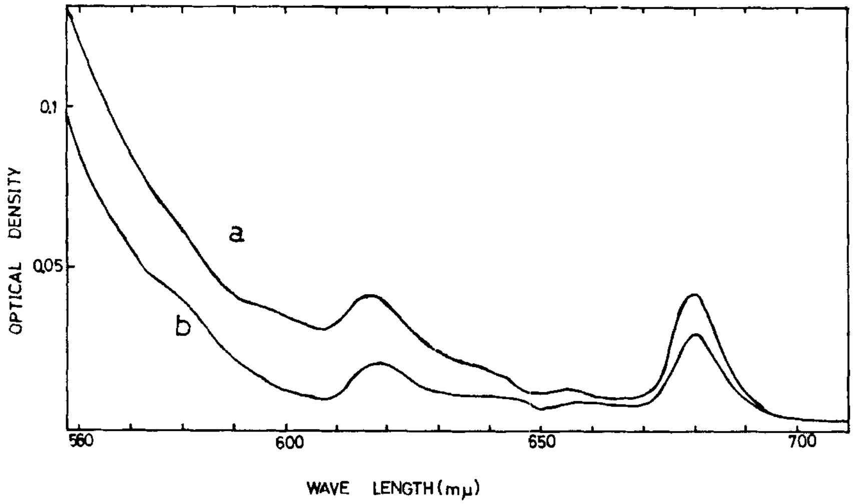

FIGURE 9 Details of the absorption spectrum shown in Figure 8 in the longer wave length region.

References

1. T. Okubo, N. Itoh, and T. Suita, *Mol. Cryst. Liq. Cryst.*, **6**, 227 (1969).
2. N. Itoh and T. Okubo, *Mol. Cryst. Liq. Cryst.*, **17**, 303 (1972).
3. U. R. Bohme and G. W. Jesse, *Chem. Phys. Letters*, **3**, 329 (1969).
4. T. Chong and N. Itoh, *Mol. Cryst. Liq. Cryst.*, **36**, 99 (1976).
5. T. Chong and N. Itoh, *J. Phys. Soc. Japan*, **35**, 518 (1973).
6. G. Dallinga, E. L. Mackor, and A. A. Verrijn Stuart, *Mol. Phys.*, **1**, 123 (1958).
7. T. Shida and I. Hanazaki, *Bull. Chem. Soc. Japan*, **43**, 646 (1970).
8. R. W. Jennings and L. K. Wilson, *Mol. Cryst. Liq. Cryst.*, **17**, 315 (1972).
9. J. A. Leone and W. S. Koski, *J. Am. Chem. Soc.*, **88**, 656 (1966).
10. I, Hanazaki and S. Nagakura, *Bull. Chem. Soc. Japan*, **38**, 1298 (1965).
11. J. M. Robertson and J. G. White, *J. Chem. Soc.*, **1947**, 358 (1947).